Table I. Speed of Sound and Isentropic Compressibility for Formic Acid

T, K	ω_s, GHz	C_s, m s^{-1}	χ_s, GPa
293.15	4.89	1297	0.487
298.15	4.87	1283	0.500
303.15	4.78	1272	0.512
307.15	4.76	1268	0.517
311.15	4.74	1264	0.522
315.15	4.68	1250	0.536
318.15	4.65	1243	0.544
338.15	4.44	1193	0.602

Table II. Speed of Sound and Isentropic Compressibility for Acetic Acid

T, K	ω_s, GHz	C_s, m s^{-1}	χ_s, GPa
293.15	4.27	1134	0.745
298.15	4.21	1119	0.768
307.15	4.17	1110	0.785
311.15	4.13	1101	0.802
315.15	4.04	1078	0.837
318.15	4.01	1071	0.854
324.15	3.94	1054	0.887
330.15	3.84	1029	0.937
332.15	3.81	1021	0.953
338.15	3.74	1004	0.992
348.15	3.65	983	1.047
353.15	3.60	971	1.080

of a study of sound velocity in associated liquids. A literature survey revealed that no one has previously reported these properties as a function of temperature.

Experimental Section

Purification of Acids. Formic, acetic, and propionic acids were obtained from Eastman Kodak. The acids were repeatedly filtered through a fritted glass with a pore size of 4.5–5.0 μm, into a fluorescence cell. The filtration was necessary in order to remove dust from the sample, which may obscure the Brillouin peaks.

Measurement of the Speed of Sound. The experimental setup has been previously published (*1*). An argon ion laser operated at 514.5 nm was focused onto the sample cell. The cell was thermostated and the temperature controlled to ±0.05 K. The scattered light was focused through a Fabry-Perot interferometer with a long focal length lens. Output of the interferometer was focused with a second lens through a pinhole onto a photomultiplier tube. The output of the photomultiplier tube was amplified and digitized and subsequently stored in an LSI 11/03 minicomputer.

The free spectral range for the acetic acid was 13.0 and 11.9 GHz for the formic and propionic acids. The sound velocities are accurate to ±2% and the isentropic compressibilities to ±3%.

Results and Discussion

The sound velocities and isentropic compressibilities for formic, acetic, and propionic acids are given in Tables I–III. The experimentally measured quantity in Brillouin light scattering is the adiabatic sound frequency, ω_s. The adiabatic sound frequency is given by the frequency shift of the Brillouin peaks from the laser frequency relative to the splitting between adjacent orders of the Brillouin spectra. The splitting between adjacent orders is the free spectral range and is used to calibrate the frequency shift of the digitized data.

The sound velocity was calculated with eq 1

$$C_s = 2\pi\omega_s/q \tag{1}$$

Table III. Speed of Sound and Isentropic Compressibility for Propionic Acid

T, K	ω_s, GHz	C_s, m s^{-1}	χ_s, GPa
293.15	4.42	1162	0.750
303.15	4.35	1145	0.777
307.15	4.33	1141	0.786
311.15	4.24	1119	0.821
315.15	4.21	1112	0.834
318.15	4.12	1089	0.873
324.15	4.08	1080	0.893
330.15	3.96	1050	0.951
332.15	3.95	1048	0.956
335.15	3.88	1031	0.993
344.15	3.86	1028	1.018
348.15	3.75	1000	1.070
353.15	3.70	998	1.103

where C_s is the sound velocity and q is the scattered wave vector, given by

$$q = (4\pi n/\lambda) \sin(\theta/2) \tag{2}$$

where n is the refractive index, λ is the wavelength of the incident light, and θ is the scattering angle. In all these measurements the scattered intensity was measured at θ equal to 90°. The refractive indices were obtained from published values (*2–4*).

A thousand data points over two spectral orders were acquired. All spectral were fitted with a nonlinear least-squares fitting routine from which the ω_s values were obtained.

The isentropic compressibility, χ_s, was calculated with

$$\chi_s = C_s^{-2}\rho^{-1} \tag{3}$$

where ρ is the density. Values for the density as a function of temperature were also obtained from the literature (*2*). The density and refractive indices were interpolated from the values given in the literature. From the given uncertainty in the reported values of density and refractive index the error in these quantities is less than 1% and does not contribute significantly to the error in the reported sound velocity. The major source of error is in the uncertainty in the free spectral range (±2%) which produces a systematic error in all data sets.

A survey of the literature revealed that the only other measurements of the sound velocity were at 293 K using ultrasonics. The values reported were 1287 m s^{-1} for formic acid (*2*), 1164 and 1150 m s^{-1} for acetic acid (*2*, *5*), and 1179 m s^{-1} for propionic acid (6) and are all within the quoted error of our values.

Registry No. Formic acid, 64-18-6; acetic acid, 64-19-7; propionic acid, 79-09-4.

Literature Cited

(1) Keegan, P. F.; Whittenburg, S. L. *J. Phys. Chem.* **1982**, *86*, 4622.
(2) Helwege, K. H. "Landolt-Bornstein: Numerical Data and Functional Relationships in Science and Technology", 6th ed.; Springer-Verlag: New York, 1967.
(3) "International Critical Tables of Numerical Data, Physics, Chemistry and Technology"; McGraw-Hill: New York, 1933.
(4) Bolt, H. G. "Beilsteins Handbuch der Organischen Chemie"; Springer-Verlag: West Berlin, 1920; Vol. 2.
(5) Lamb, J.; Pinkerton, J. M. M. *Proc. R. Soc. London, Ser. A* **1949**, *199*, 114.
(6) Lamb, J.; Huddart, D. H. A. *Trans. Faraday Soc.* **1950**, *46*, 540.

Received for review December 20, 1982. Accepted April 29, 1983. We acknowledge the Research Corp. UNO Research Council, and the University of New Orleans Computer Research Center for support of this research.

Table I. Properties Characterizing the Pure Components at 25 °C

substances		ρ, g cm^{-3}	n_D	$10^6\chi_M$, cgs mol^{-1}	$10^{24}\alpha$[a]
MIK	exptl	0.7963	1.39361	−70.71	11.914
	lit.	0.7961 (9)	1.3933 (9)	−69.31 (10)	
B_1	exptl	0.8060	1.39741	−56.52	8.785
	lit.	0.8060 (9)	1.3973 (9)	−56.53 (10)	
B_2	exptl	0.8025	1.39530	−57.67	8.782
	lit.	0.8026 (9)	1.3950 (9)	−57.68 (10)	
B_3	exptl	0.7980	1.39389	−57.70	8.804
	lit.	0.7978 (9)	1.3939 (9)	−57.70 (10)	

[a] Calculated from the Lorentz-Lorenz equation.

Table II. Experimental and Calculated Values from Eq 2 of the Diamagnetic Molar Susceptibility

MIK + B_1			MIK + B_2			MIK + B_3		
	$-10^6\chi_M$[a]			$-10^6\chi_M$[a]			$-10^6\chi_M$[a]	
x_{MIK}	exptl	calcd	x_{MIK}	exptl	calcd	x_{MIK}	exptl	calcd
0.0000	56.52	55.61	0.0000	57.67	55.60	0.0000	57.70	55.66
0.1016	57.39	57.41	0.1028	57.99	57.42	0.0923	58.73	57.29
0.1952	58.41	59.06	0.2131	59.26	59.37	0.1970	59.88	59.14
0.2965	59.73	60.86	0.2934	60.10	60.80	0.2936	61.03	60.85
0.3834	60.83	62.40	0.4034	61.36	62.75	0.4025	62.41	62.77
0.5062	62.64	64.57	0.5008	62.75	64.47	0.4990	63.66	64.48
0.6055	64.09	66.34	0.6013	64.30	66.26	0.6026	65.07	66.31
0.6965	65.39	67.95	0.6991	65.46	67.99	0.6973	66.45	67.98
0.7962	67.11	69.72	0.7979	67.04	69.74	0.7984	67.87	69.77
0.8984	68.76	71.53	0.8998	68.82	71.55	0.8906	69.08	71.39
1.0000	70.71	73.33	1.0000	70.71	73.33	1.0000	70.71	73.33

[a] Units: cgs mol^{-1}.

Table III. Coefficients for Eq 4 Determined by the Method of Least Squares

	$10^6 a_j$					
system	a_0	a_1	a_2	a_3	a_4	σ_x
MIK + B_1	−0.007 31	7.453 61	−18.4853	20.2790	−9.2207	0.05
MIK + B_2	0.043 16	10.584 6	−28.5059	33.5176	−15.668	0.1
MIK + B_3	−0.017 96	2.878 69	−4.20117	0.92212	0.43212	0.04

All systems show positive excess molar susceptibility (see Figure 1) over the whole concentration range. This is a consequence of the breaking of hydrogen bonds in the butyl alcohols when MIK is added. In these systems, the dispersion forces are dominant, which is in agreement with our previous conclusions (*2*). The rupture of O–H···O bonds in the alcohols leads to large positive values of χ_M^E.

Complexes between solute and solvent have also been investigated by methods based upon the deviation from additivity of the refractive indexes (*11*, *12*). For mixtures of two liquids, A and D, the additivity refractive index of the solutions (n_a), calculated as if there were no intermolecular interactions, would be

$$n_a = [\varphi_A n_A + (1 - \varphi_A) n_D] \quad (6)$$

For many of the binary systems, in which spectroscopic or other methods indicate that molecular interaction occurs, it is found that $\Delta n = n_{sol} - n_a > 0.004$. Therefore, these authors conclude that $\Delta n > 0.004$ is indicative of complex formation. For our systems, we have observed that Δn's values never reached $\Delta n = 0.004$. This is an indication that no intermolecular complexes are formed.

All alcohols are associated in the pure state, the energy of the hydrogen bonds in our systems being as follow: $B_1 > B_3 > B_2$. Then, it is easier to break the hydrogen bond in B_2 than in other alcohols, therefore yielding the greatest positive deviation for the excess magnetic susceptibility.

The relative position between the curves for MIK + B_1 and MIK + B_3 could be explained by a stronger dipole–dipole interaction in the mixture MIK + B_1 than in MIK + B_3 because B_3 has a methyl group on the α carbon.

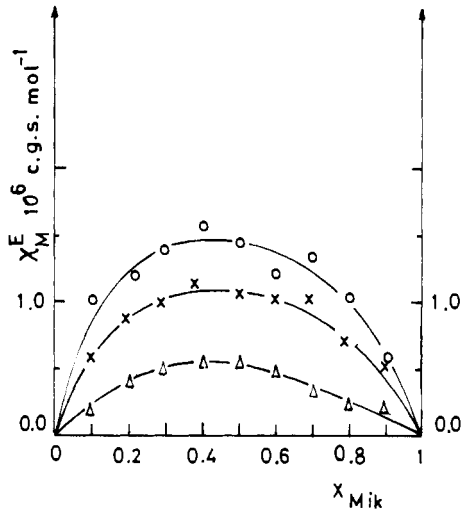

Figure 1. Excess molar susceptibility χ_M^E against mole fraction of the MIK: (×) MIK + B_1; (○) MIK + B_2; and (△) MIK + B_3.

Glossary

χ_M^E	excess molar diamagnetic susceptibility, cgs mol^{-1}
χ_M	molar diamagnetic susceptibility of the solution, cgs mol^{-1}
χ_1, χ_2	molar diamagnetic susceptibilities of the pure components
x_1, x_2	mole fraction of the pure components
f	constant in eq 1 (= −3.46 × 10^6)
n_i'	effective number of electrons
n_i	valence electrons of the component i

n_{i0} characteristic constant for each family of substances
α_i molecular polarizability of the component i, cm^3 mol^{-1}
a_j polynomial coefficients in eq 4
n_A, n_D refractive indexes of A and D in eq 6
φ_A volume fraction of the component A in eq 6
n polynomial degree
ρ density of the solution, g cm^{-3}

Registry No. Methyl isobutyl ketone, 108-10-1; *sec*-butyl alcohol, 78-92-2; isobutyl alcohol, 78-83-1; *n*-butyl alcohol, 71-36-3.

Literature Cited

(1) Gopalakrishnan, R. *J. Prakt. Chem.* **1971**, *6*, 1178.
(2) Riggio, R.; Ramos, J. F.; Hernandez Ubeda, M.; Espíndola, J. A. *Can. J. Chem.* **1981**, *59*, 3305.
(3) Kirkwood, J. G. *Phys. Z.* **1931**, *33*, 57.
(4) Sólimo, H. N.; Alonso, S. del V.; Katz, M. *Can. J. Chem.* **1979**, *57*, 768.
(5) Boyer-Donzelot, M. Doctoral Thesis, University of Nancy I, Nancy, France, 1974.
(6) Boyer-Donzelot, M.; Barriol, J. *Bull. Soc. Chim. Fr.* **1973**, *11*, 2972.
(7) Robertson, G. R. *Ind. Eng. Chem., Anal. Ed.* **1939**, *11*, 464.
(8) Radi, H. S. *J. Phys. Chem.* **1973**, *77*, 424.
(9) Riddick, J. A.; Bunge, W. B. "Organic Solvents", 3rd ed.; Wiley-Interscience: New York, 1970; Vol. II.
(10) Weast, J. "Handbook of Chemistry and Physics", 58th ed.; CRC Press: Cleveland, OH, 1977.
(11) Voronkov, M. G.; Deich, A. Y. *Teor. Eksper. Khim., Akad., Nauk. Ukr. SSR.* (*Engl. Transl.*) **1965**, *1*, 443.
(12) Voronkov, M. G.; Deich, A. Y.; Akatova, E. V. *Khim. Geterotsikl. Soedin., Akad. Nauk. Lat. SSR.* (*Engl. Transl.*) **1966**, *2*, 5.

Received for review May 6, 1982. Revised manuscript received March 22, 1983. Accepted April 7, 1983. Support of this research by the INENCO of the Universidad Nacional de Salta-República Argentina is greatly appreciated.

Thermodynamic Properties of Isobutane in the Critical Region

J. M. H. Levelt Sengers,*† B. Kamgar-Parsi,‡ and J. V. Sengers†‡

Thermophysics Division, National Bureau of Standards, Washington, D.C. 20234, and Institute for Physical Science and Technology, University of Maryland, College Park, Maryland 20742

For geothermal applications, a scaled fundamental equation has been formulated in order to represent and tabulate the thermodynamic properties of isobutane in the critical region. In the supercritical range, the surface joins smoothly with that of Waxman and Gallagher, to which it is a complement. The range of the surface is 405–438 K in temperature, 150–290 kg/m³ in density. The critical constants are T_c = 407.84 ± 0.02 K, ρ_c = 225.5 ± 2 kg/m³, P_c = 3.629 ± 0.002 MPa. Comparisons are made with the *PVT* data of Beattie et al., and of Waxman, and also with the formulations of Waxman and Gallagher, and of Goodwin and Haynes.

Introduction

Isobutane has been proposed as the working fluid in binary geothermal power cycles. In this application, the fluid would pass through the heat exchanger at a pressure exceeding the critical pressure (P_c = 3.63 MPa), while it is heated from ambient to supercritical temperatures (T_c = 408 K). The initial state of the fluid entering the turbine would be a supercritical pressure and temperature, while the density would be somewhat below the critical. The gas would then expand isentropically along a path that, preferably, should remain within the one-phase vapor region. Kestin and Khalifa (*1*, *2*) pointed out that the then-existing formulations of the thermodynamic properties of isobutane were of insufficient reliability for design of an efficient cycle. The lack of reliability was due, to a considerable extent, to sparsity and inconsistency of the thermodynamic data. Since then, the situation has been remedied, at least to a good extent, by the acquisition of new data on the vapor pressure and on *PVT* of the vapor and supercritical phase by Waxman et al. (*3–6*), and on *PVT* of the liquid by Haynes (*7*). These new accurate data permitted Waxman et al. to select the bodies of reliable data.

It was decided to approach the formulation of the thermodynamic surface in two steps. Waxman and Gallagher (*5*, *6*) adapted the free energy model developed by Haar and coworkers (*8*) to represent the thermodynamic properties of isobutane up to 40 MPa and from 250 to 700 K with the exclusion of a region around the critical point the size of which is

$$0.985 \leq T_c/T \leq 1.015 \quad \text{i.e., } 401.8 \leq T \leq 414 \text{ K}$$

$$0.7 \leq \rho_c/\rho \leq 1.3 \quad \text{i.e., } 173.4 \leq \rho \leq 322 \text{ kg/m}^3 \quad (1)$$

The thermodynamic surface that we present here is valid in the range

$$405 \leq T \leq 438 \text{ K}$$

$$150 \leq \rho \leq 290 \text{ kg/m}^3 \quad (2)$$

and thus supplements the surface of Waxman et al. in most of the excluded range. The model that we use is that of revised and extended scaling, as developed according to the modern theory of critical phenomena (*9*). We have applied this model successfully to the thermodynamic properties of light and heavy water (*10*, *11*) in the critical region. Here, however, we use a somewhat different approach toward determining the model parameters. We obtained most of our parameter values by a fit to the experimental *PVT* data of Beattie et al. (*12*, *13*), which were recently validated by Waxman (*6*). There are a large number of *PVT* data in a very narrow temperature region, from 407.8 to 408.3 K, around the critical point; the only other data available in our range are on the 423.17 K isotherm. It is clear that temperature derivatives of the surface cannot be reliably taken if the surface is based on only two isotherms. We therefore supplemented the experimental data with *PVT* points generated from the surface of Waxman et al. in a range in which the surface is valid. This practice has yielded three benefits. It has helped pinpoint our surface, has ensured a smooth crossover to the analytic surface along most of the boundary, and has provided the entire analytic "background" for the caloric parameters, for which, in the case of isobutane, no experimental information is available.

The critical-point parameters incorporated in the scaled equation differ from those reported by Beattie et al. (*12*). If the critical parameters are freely adjusted in the fit to a scaled equation, the value of the critical temperature falls as much as

† National Bureau of Standards.
‡ University of Maryland.